Theory of Square Wave Voltammetry of Two Reversible Electrode Reactions Connected by The Reversible Chemical Reaction

Šebojka Komorsky-Lovrić and Milivoj Lovrić

Divkovićeva 13, Zagreb 10090, Croatia

mlovric@irb.hr

Abstract

A theory of the mechanism that consists of two reversible electrode reactions coupled by kinetically controlled reversible chemical reaction is developed for square wave voltammetry on stationary planar electrode. The influences of frequency and the concentration of electro-inactive chemical reactant on the responses are investigated for thermodynamically stable intermediate. The limits of three types of responses are calculated and the formula for the estimation of the forward rate constant of chemical reaction is proposed.

Keywords: ECE Mechanism; Square Wave Voltammetry; Theory; Kinetics; Equilibrium Conditions.

Introduction

A nine-member square scheme [1 - 3] is theoretical representation of two-electron, two-proton electrode reactions of many organic compounds, such as catechols [4] and quinones [5]. A special case of this scheme is the ECE mechanism in which two electrode reactions are connected by the chemical reaction in such a way that the reactant and product of chemical reaction are the product of the first electrode reaction and the reactant of the second one, respectively [6 - 12]. The theory of this mechanism is developed for chronoamperometry [13], polarography [14] and voltammetry [15]. In square wave voltammetry, the theory is developed either for totally irreversible chemical reaction [16 - 19], or for the chemical reaction that is permanently in the equilibrium [20, 21]. The response depends on chemical rate constant in the first case and on thermodynamic constant in the second one. In this paper a general model of kinetically controlled reversible chemical reaction is described that enables the definition of conditions under which the ECE mechanism can be considered as being reversible, or totally irreversible.

Model

Two reversible electrode reactions coupled by the kinetically controlled reversible chemical reaction are investigated:

$$A \leftrightarrow B^+ + e^- \tag{1}$$

$$B^+ + X^- \leftrightarrow E \tag{2}$$

$$E \leftrightarrow F^+ + e^- \tag{3}$$

On the stationary, planar electrode the mass transport can be described by the semi-infinite diffusion model. If the reagent X^- is present in great excess, the variation of its concentration can be neglected. The model is solved by the following substitutions:

$$c_{Int} = c_B + c_E \tag{4}$$

$$c_H = Kc_X^* c_B - c_E \tag{5}$$

Its mathematical representation are the following differential equations and boundary conditions:

$$\partial c_A/\partial t = D\,\partial^2 c_A/\partial x^2 \tag{6}$$

$$\partial c_{Int}/\partial t = D\,\partial^2 c_{Int}/\partial x^2 \tag{7}$$

$$\partial c_H/\partial t = D\,\partial^2 c_H/\partial x^2 - \varepsilon\,c_H \tag{8}$$

$$\partial c_F/\partial t = D\,\partial^2 c_F/\partial x^2 \tag{9}$$

$$t = 0,\ x \geq 0: \qquad c_A = c_A^*,\quad c_B = c_E = c_F = 0,\ c_X = c_X^* \tag{10}$$

$$t > 0,\ x \to \infty: \qquad c_A \to c_A^*,\ c_X \to c_X^*,\ c_B \to 0 \qquad c_E \to 0,\ c_F \to 0 \tag{11}$$

$$x = 0: \qquad c_X = c_X^* \tag{12}$$

$$c_{B,x=0} = c_{A,x=0}\, exp(F(E - E_1^0)/RT) \tag{13}$$

$$c_{F,x=0} = c_{E,x=0}\, exp(F(E - E_2^0)/RT) \tag{14}$$

$$D(\partial c_A/\partial x)_{x=0} = I_1/FS \tag{15}$$

$$D(\partial c_{Int}/\partial x)_{x=0} = (I_2 - I_1)/FS \tag{16}$$

$$D(\partial c_H/\partial x)_{x=0} = -Kc_X^* I_1/FS - I_2/FS \tag{17}$$

$$D(\partial c_F/\partial x)_{x=0} = -I_2/FS \tag{18}$$

Here, $\varepsilon = k_b(1 + Kc_X^*)$ and $K = k_f/k_b$. The meanings of other symbols are reported in Table 1.

Table 1

Meanings of symbols

c_A, c_B, c_E, c_F		Concentrations of species A, B$^+$, E and F$^+$
	c_A^*, c_X^*	Concentrations of species A and X$^-$ in the bulk of solution
	c_{Int}, c_H	Concentrations of substitutions Int and H
	D	Common diffusion coefficient
	dE	Potential step
	E	Electrode potential
	E_1^0, E_2^0	Standard potentials of the first and the second electrode reactions
	E_p	Peak potential
	E_{SW}	Square wave amplitude
	F	Faraday constant
	f	Frequency

I_1, I_2	Currents of the first and the second electron transfers
K	Equilibrium constant of the chemical reactions
k_f, k_b	Rate constants of reversible chemical reaction
R	Gass constant
S	Electrode surface area
T	Temperature
t	Time
x	Distance perpendicular to electrode surface

Differential equations are solved by the numerical method [22, 23]. The solution is the system of recursive formulae for the dimensionless current $\Phi_k = I_k (FSc_A^*)^{-1}(Df)^{-1/2}$, where k = 1 or 2. The sum $\Phi = \Phi_1 + \Phi_2$ is reported as a function of electrode potential.

$$\Phi_{2,m} = -z_8 z_7^{-1} + z_9 z_7^{-1} \sum_{j=1}^{m-1} \Phi_{2,j} S_{m-j+1} + z_{10} z_7^{-1} \sum_{j=1}^{m-1} \Phi_{2,j} P_{m-j+1} + z_{11} z_7^{-1} \sum_{j=1}^{m-1} \Phi_{1,j} S_{m-j+1} + z_{12} z_7^{-1} \sum_{j=1}^{m-1} \Phi_{1,j} P_{m-j+1} \tag{19}$$

$$\Phi_{1,m} = z_8 + z_1 z_5^{-1} \sum_{j=1}^{m} \Phi_{2,j} S_{m-j+1} - z_2 z_5^{-1} \sum_{j=1}^{m} \Phi_{2,j} P_{m-j+1} - z_{13} \sum_{j=1}^{m-1} \Phi_{1,j} S_{m-j+1} - z_3 z_5^{-1} \sum_{j=1}^{m-1} \Phi_{1,j} P_{m-j+1} \tag{20}$$

$$u_1 = \sqrt{2/\pi}/5$$

$$z_1 = u_1^{-1}(1 + Kc_X^*)^{-1} \tag{21}$$

$$z_2 = (1 + Kc_X^*)^{-3/2} \kappa_b^{-1/2} \tag{22}$$

$$z_3 = Kc_X^* z_2 \tag{23}$$

$$z_4 = Kc_X^* z_1 \tag{24}$$

$$z_5 = z_1 + u_1^{-1} exp(F(E - E_1^0)/RT) + z_3 P_1 \tag{25}$$

$$z_6 = [z_4 + z_3 P_1] exp(F(E - E_2^0)/RT) \tag{26}$$

$$z_7 = z_5^{-1}(z_1 - z_2) - z_6^{-1}[u_1^{-1} + (z_4 + z_2 P_1) exp(F(E - E_2^0)/RT)] \tag{27}$$

$$z_8 = z_5^{-1} exp(F(E - E_1^0)/RT) \tag{28}$$

$$z_9 = u_1^{-1} z_6^{-1} + z_4 z_6^{-1} exp(F(E - E_2^0)/RT) - z_1 z_5^{-1} \tag{29}$$

$$z_{10} = z_2 z_6^{-1} exp(F(E - E_2^0)/RT) + z_2 z_5^{-1} \tag{30}$$

$$z_{11} = z_{13} - z_4 z_6^{-1} exp(F(E - E_2^0)/RT) \tag{31}$$

$$z_{12} = z_3 z_6^{-1} exp(F(E - E_2^0)/RT) + z_3 z_5^{-1} \tag{32}$$

$$z_{13} = [z_1 + u_1^{-1} exp(F(E - E_1^0)/RT)]/z_5 \tag{33}$$

$$\kappa_b = k_b/f \tag{34}$$

$$P_i = erf\sqrt{\kappa_b(1 + Kc_X^*)qi} - erf\sqrt{\kappa_b(1 + Kc_X^*)q(i-1)} \tag{35}$$

$$q = 1/50 \tag{36}$$

$$s_p = \sqrt{p} - \sqrt{p-1} \tag{37}$$

$$m = 1, 2, 3 \dots \tag{38}$$

Results and Discussion

Theoretical dimensionless square wave voltammograms of ECE mechanism depend on the difference between standard potentials of two electrode reactions. If $E_2^0 - E_1^0 > 0.15$ V and both electron transfers are fast and reversible, the response consists of two peaks [24]. Furthermore, the voltammograms depend on the product of equilibrium constant of chemical reaction ($K = k_f/k_b$) and the bulk concentration of species X^-. This product defines the ratio of equilibrium concentrations of the product B^+ and the second reactant E. Finally, the response depends on the ratio of backward rate constant and square wave frequency.

A)
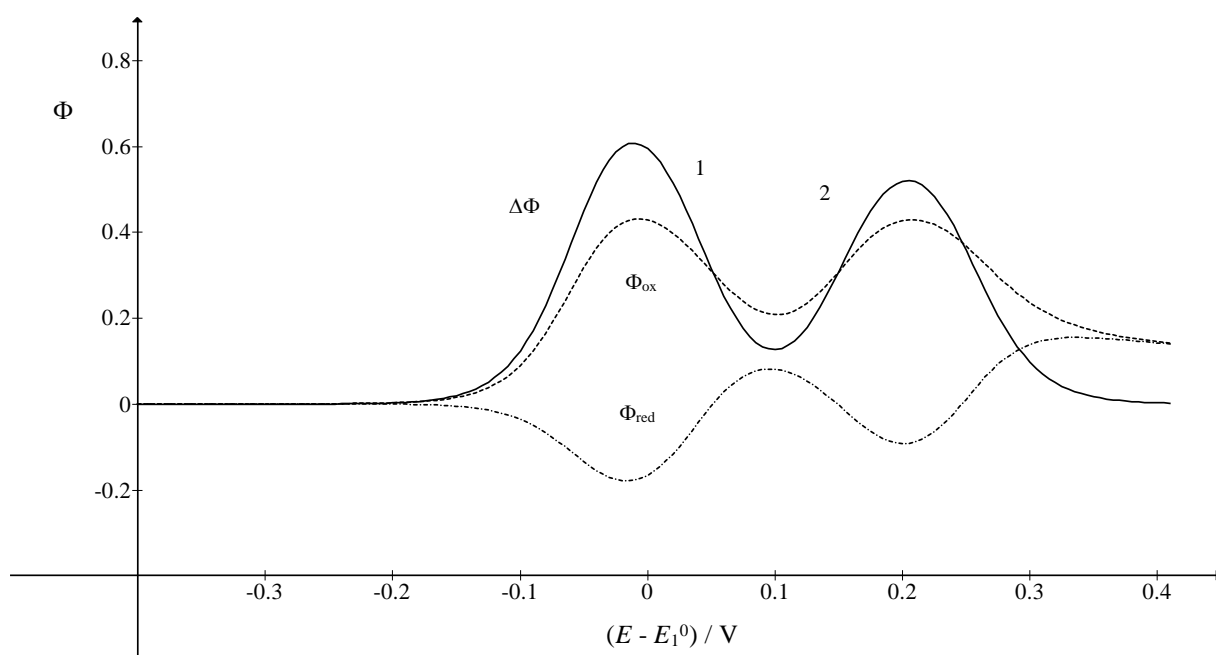
B)
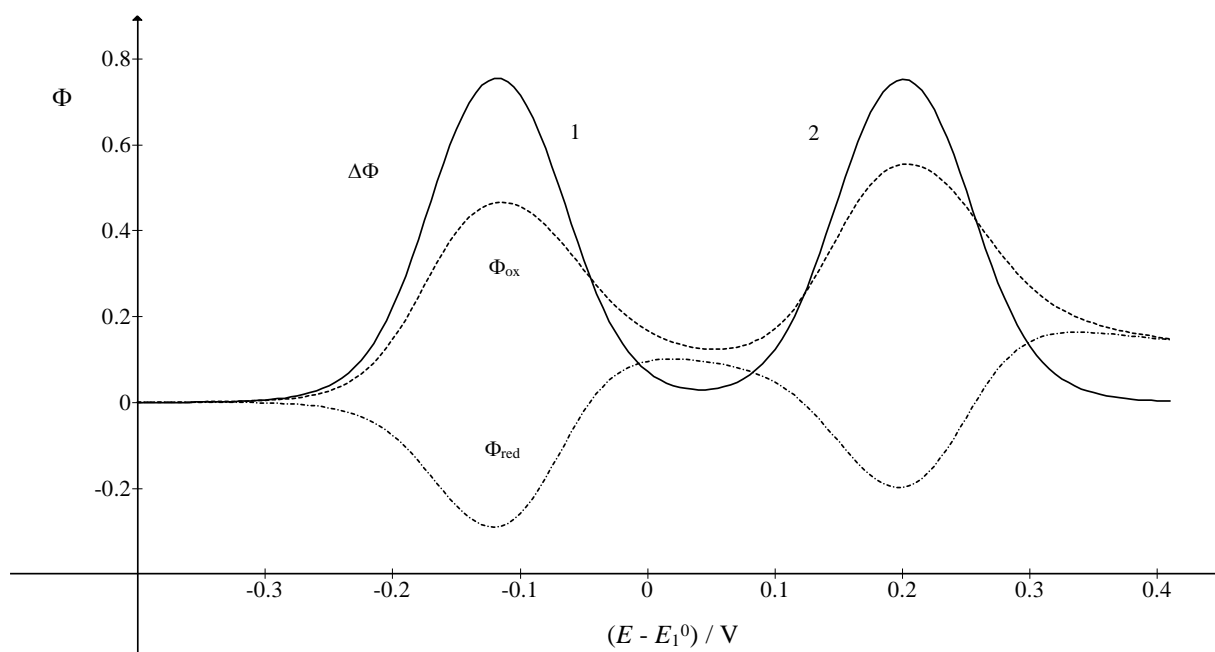
Fig. 1 Square wave voltammograms of ECE mechanism. $E_2^0 - E_1^0 = 0.2$ V, E_{SW} = 50 mV, dE = 5 mV, Kc_X^* = 100 and k_b/f = 10^{-3} (A) and 10^4 (B). The net current ($\Delta\Phi = \Phi_{ox} - \Phi_{red}$) and its forward ($\Phi_{ox}$) and backward ($\Phi_{red}$) components are shown.

Two examples of ECE voltammograms are shown in Fig. 1. They correspond to the case of thermodynamically stable intermediate and the chemical reaction that favours the substance E. If the dimensionless backward rate constant is relatively low (k_b/f = 10^{-3}), the first net peak current is higher than the second one ($\Delta\Phi_{p,1}$ = 0.608 and $\Delta\Phi_{p,2}$ = 0.521) and the net peak potentials are -0.010 V and 0.205 V *vs.* E_1^0, respectively. If the ratio k_b/f is much higher, two peak currents are almost equal ($\Delta\Phi_{p,1}$ = 0.755 and $\Delta\Phi_{p,2}$ = 0.752), but the peak potentials are -0.120 V and 0.200 V *vs.* E_1^0. The difference in the first net peak currents can be explained by the change in their backward components. In Fig. 1A the minimum of this component is equal to -0.18, while in Fig. 1B this minimum decrease to -0.29. The origin of backward component is the reduction of the product B$^+$. So, it is proportional to the concentration of this species. The chemical reaction may consume this product and then the backward component of current is diminished. However, if the backward rate constant of chemical reaction is very high, the concentration of the product B$^+$ is restored by decomposition of the second reactant E. In this case the first minimum of the backward component of current deepens. The lower value of the first net peak potential is caused by the formation energy of the reactant E.
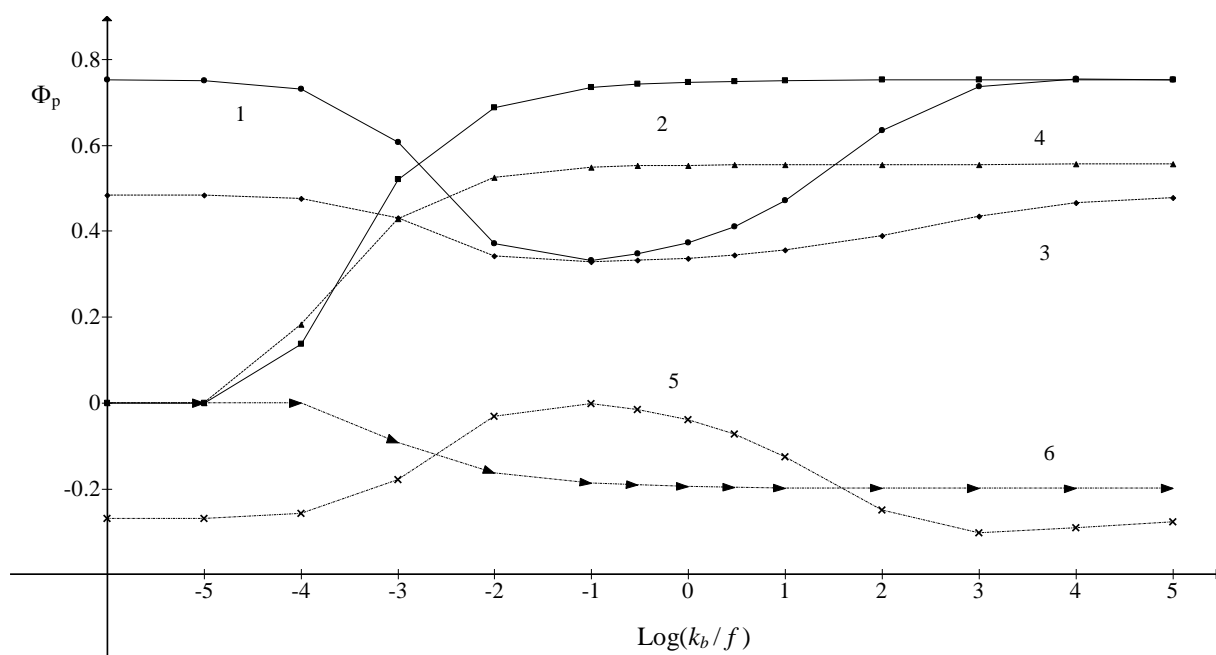
Fig. 2 Dependence of peak currents on the logarithm of dimensionless backward rate constant: $\Delta\Phi_{p,1}$ (1), $\Delta\Phi_{p,2}$ (2), $\Phi_{p,ox,1}$ (3), $\Phi_{p,ox,2}$ (4), $\Phi_{p,red,1}$ (5) and $\Phi_{p,red,2}$ (6). All other data are as in Fig. 1.

The influence of the variation of square wave frequency on peak currents of ECE voltammograms is shown in Fig. 2. The results can be divided in three parts. If $\log(k_b/f) < -5$ the response consists of a single peak that corresponds to the first electrode reaction. The net peak potential is equal to the first standard potential. Within the range $-5 < \log(k_b/f) < 4$ the response is controlled by the kinetics of chemical reaction. The first peak current and its components are diminished for $\log(k_b/f) \leq -1$, but augmented for higher values of this argument. The first peak potential changes from zero to -0.120 V *vs.* E_1^0 in this range. The second peak current is sigmoidal function of $\log(k_b/f)$, but its potential is independent of this ratio. Finally, if $\log(k_b/f) > 4$ the both net peak currents are equal and the chemical reaction is permanently in the equilibrium. In the first and the third part of these results the real net peak currents depend linearly on the square root of frequency, but not in the second part in which the dimensionless peak currents $\Delta\Phi_{p,1}$ and $\Delta\Phi_{p,2}$ are also functions of the frequency.

A)

B)
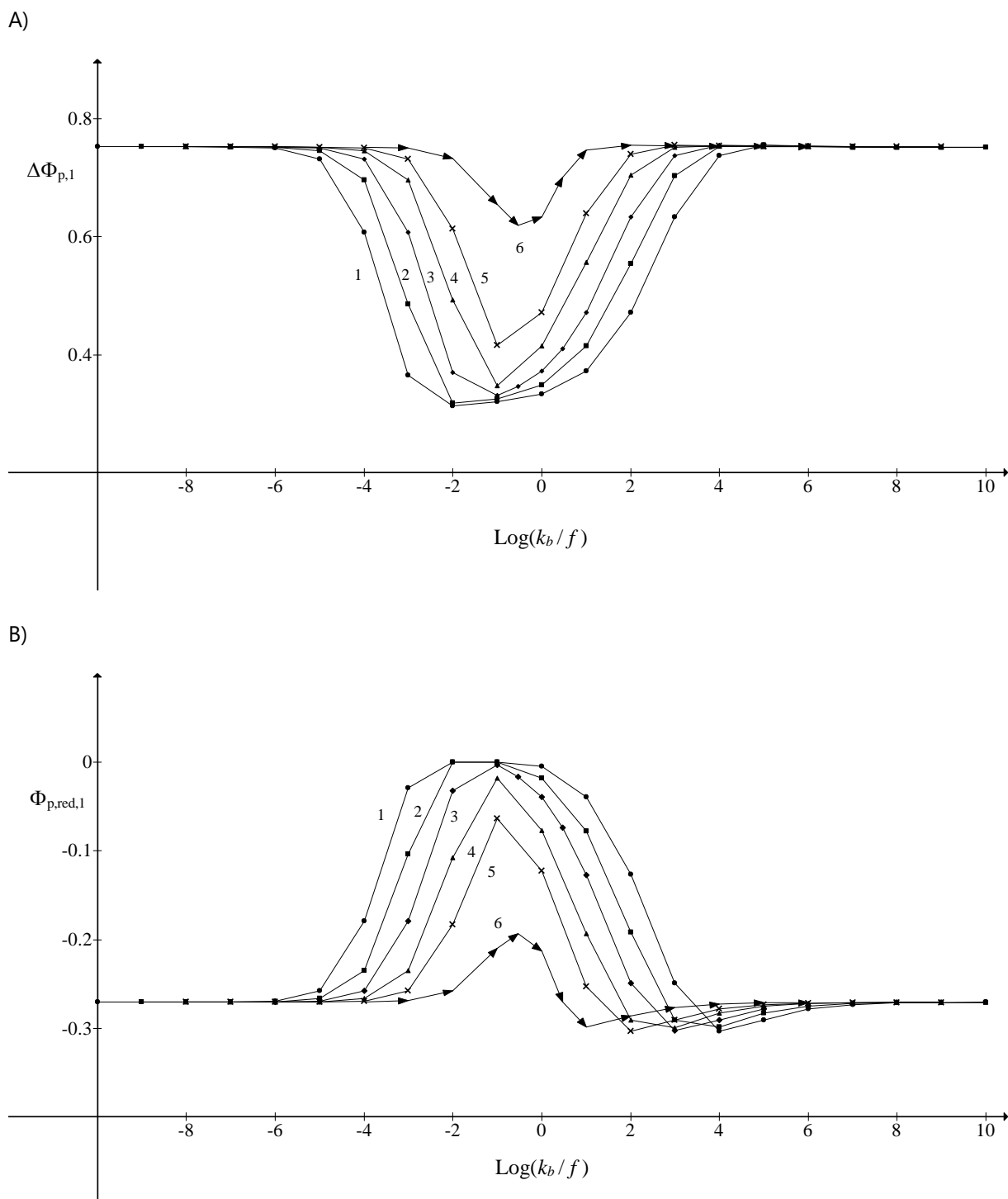
Fig. 3 Dependence of the first net peak current (A) and the first minimum of the backward component (B) on the logarithm of k_b/f ratio. $Kc_X^* = $ 1000 (1), 300 (2), 100 (3), 30 (4), 10 (5) and 1 (6). All other data are as in Fig. 1.

The relationships that are shown in Fig. 2 depend on the bulk concentration of the species X⁻, as can be seen in Figs. 3 and 4. The first one shows the depression of the first net peak current and the diminution of its backward component. One can notice that the range of kinetically controlled responses widens with the increasing product Kc_X^*. Also, if the frequency is constant and the bulk concentration of X⁻ is increased, the first peak appears less reversible, i.e. its net peak current is smaller and the minimum of backward component is shallower. At very high

values of the ratio k_b/f the first dimensionless net peak current becomes independent of the frequency. The critical frequency and the product Kc_X^* are related by the following equation:

$$\text{Log}(k_b/f)_{\text{crit}} = \text{Log}(Kc_X^*) + 2 \tag{39}$$

If this condition is satisfied, both net peak potentials are independent of frequency.
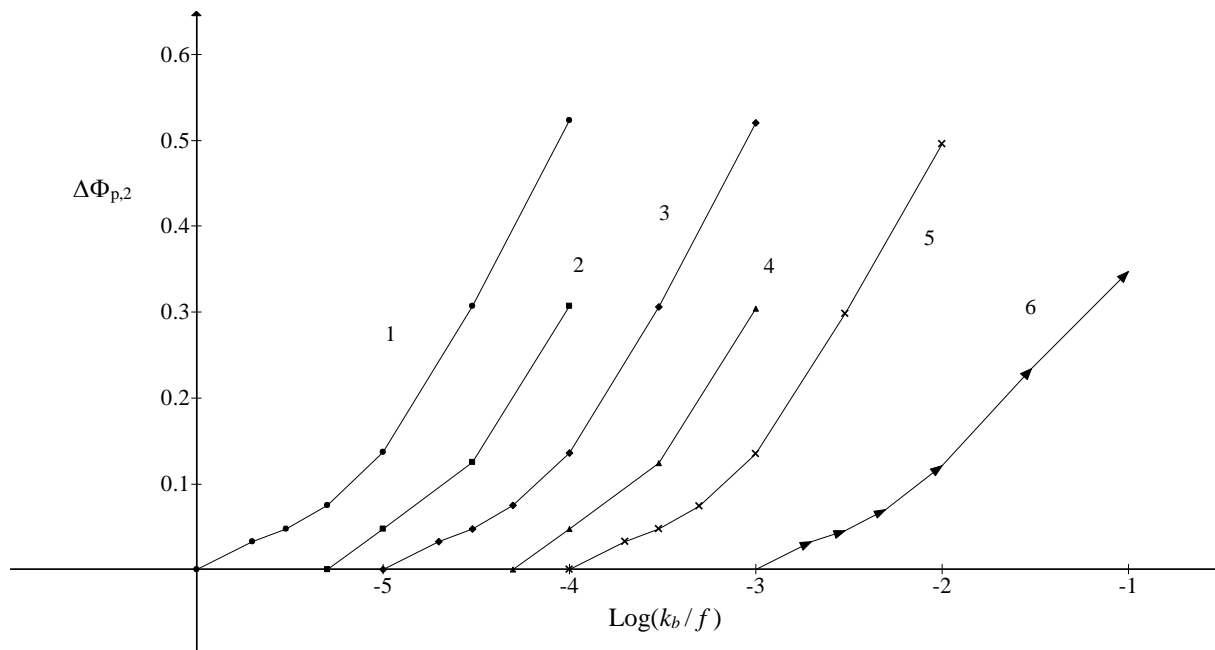
Fig. 4 Dependence of the second net peak current on the logarithm of k_b/f ratio. $Kc_X^* = 1000$ (1), 300 (2), 100 (3), 30 (4), 10 (5) and 1 (6). All other data are as in Fig. 1.

Fig. 4 shows the relationships between the second dimensionless net peak current and square wave frequency, for various concentrations of X$^-$. As the frequency is increased, the second peak eventually disappears. The critical frequency depends on the product Kc_X^*:

$$\text{Log}(k_b/f)_{\text{crit}} = -\text{Log}(Kc_X^*) - 3 \tag{40}$$

So, the forward rate constant of chemical reaction can be estimated by the variation of frequency:

$$k_f = 10^{-3} f_{\text{crit}} / c_X^* \tag{41}$$
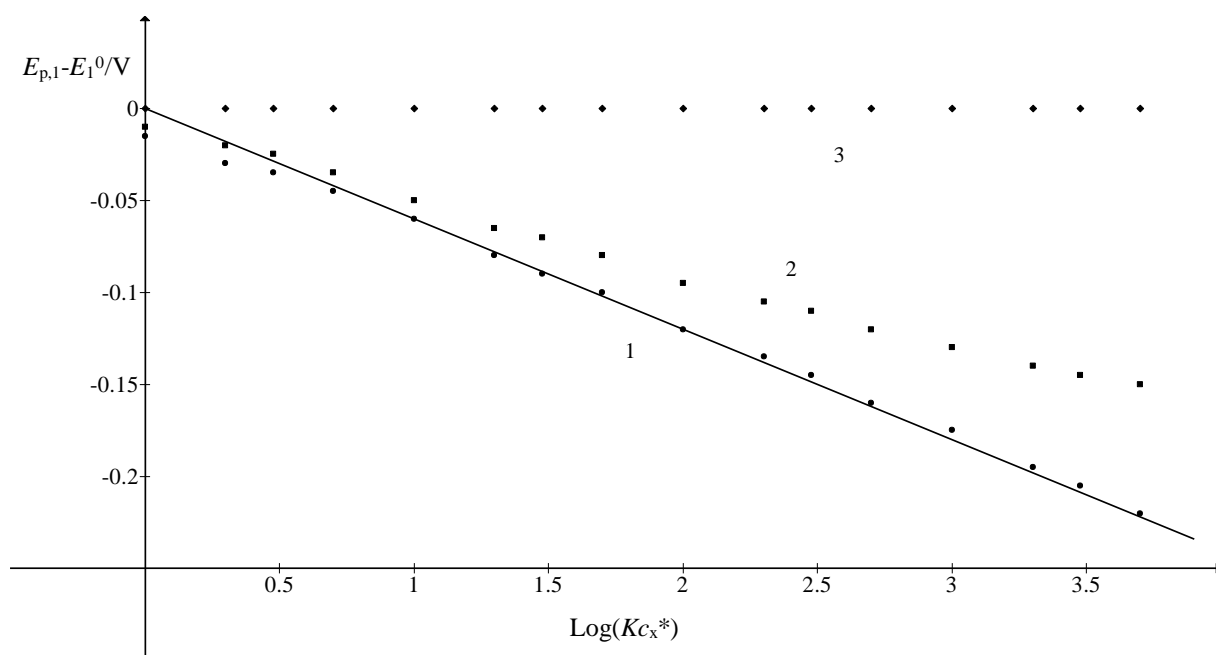
Fig. 5 Dependence of the first peak potential on the logarithm of Kc_X^* product; k_b/f = 10^9 (1), 1 (2) and 10^{-6} (3), All other data are as in Fig. 1.

The equilibrium constant can be determined by the variation of the bulk concentration of X⁻ if the measurement can be performed at the frequency at which the chemical reaction is apparently in the equilibrium. Under this condition the first net peak potential depends linearly on the logarithm of the product Kc_X^*, with the slope - 0.059 V. This is shown in Fig. 5. If the response is controlled by the kinetics of chemical reaction, the relationship between $E_{p,1}$ and $\log(Kc_X^*)$ is not linear and the slopes of local segments are smaller than the limiting one. Finally, curve 3 shows that in the case of very slow chemical reaction, the first peak potential does not depend on the concentration of species X⁻.
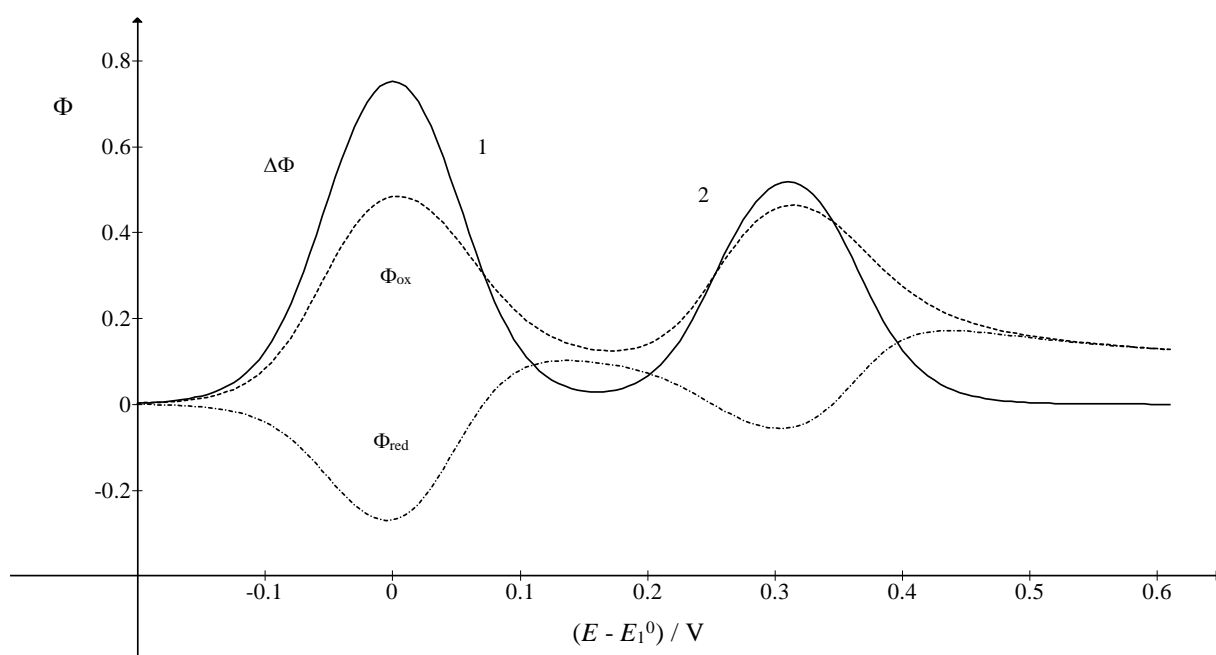
Fig. 6 Square wave voltammogram of ECE mechanism. $Kc_X^* = 0.01$ and $k_b/f = 10^4$. All other data are as in Fig. 1.

Fig. 6 shows theoretical response of ECE mechanism in which chemical reaction does not prefer the second redox couple. First dimensionless peak current and its potential are independent of kinetic parameters. The second net peak potential is 0.310 V vs. E_1^0, which is higher than the second standard potential. This additional energy is needed for chemical reaction. For $Kc_X^* = 10^{-2}$ the second peak appears if $k_b/f > 2$. This is shown in Fig. 7. The second net peak current becomes independent of the ratio k_b/f if this parameter is higher than 10^7.
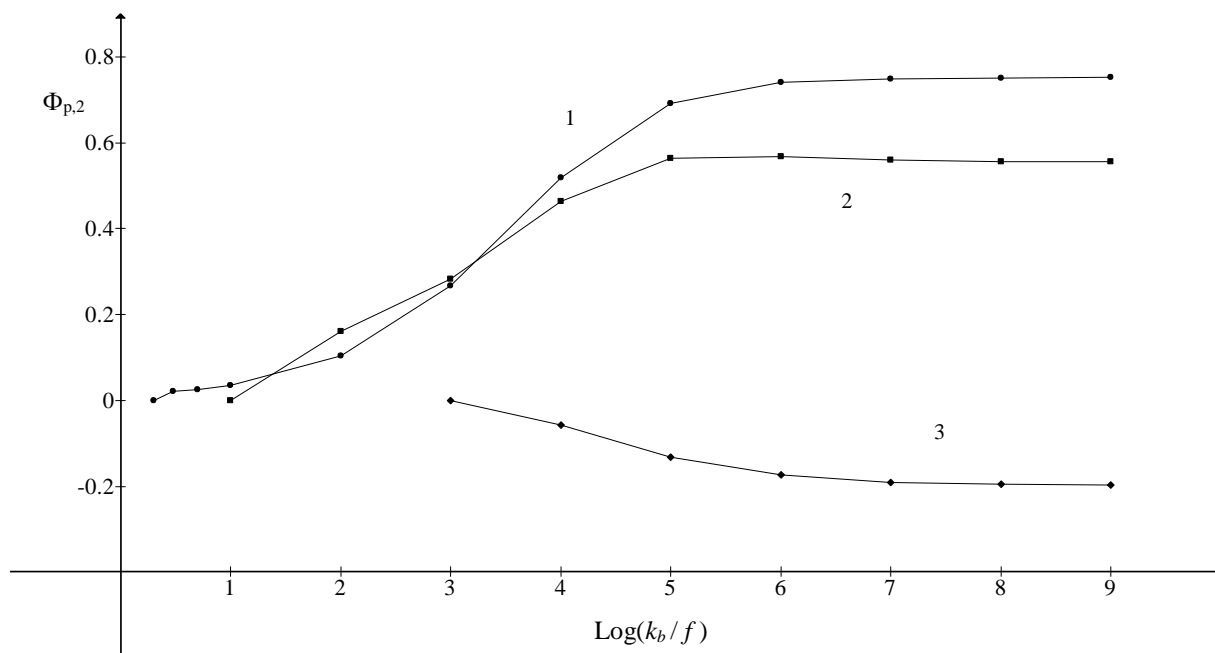
Fig. 7 Dependence of the second net peak current (1), the second maximum of the forward component (2) and the second minimum of the backward component (3) on the logarithm of k_b/f ratio. $Kc_X^* = 0.01$ and all other data as in Fig. 1.

The influence of the product Kc_X^* on these two critical parameters is shown in Fig. 8. The minimum ratio k_b/f that is required for the appearance of the second peak is higher than the one that is shown in Fig. 4. The relationship reported in Fig. 8A can be approximated by the straight line: $\log(k_b/f)_{crit} = -1.43 \log(Kc_X^*) - 3$. This means that the simple eq. (41) does not apply if $Kc_X^* < 10^{-1}$. The linear relationship that is shown in Fig. 8B satisfies the following equation:

$$\text{Log}(k_b/f)_{crit} = -2 \log(Kc_X^*) + 3 \tag{42}$$

If this condition is satisfied, the second net peak potential depends linearly on the logarithm of the product Kc_X^*, with the slope -0.059 V.

A)
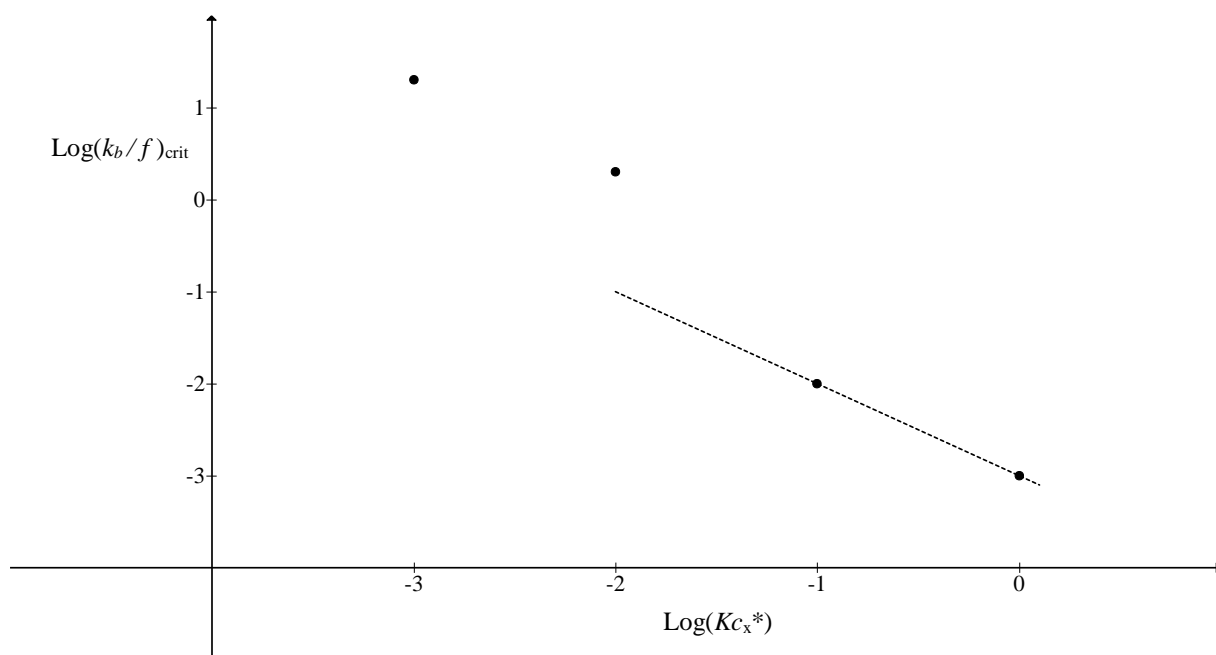
B)
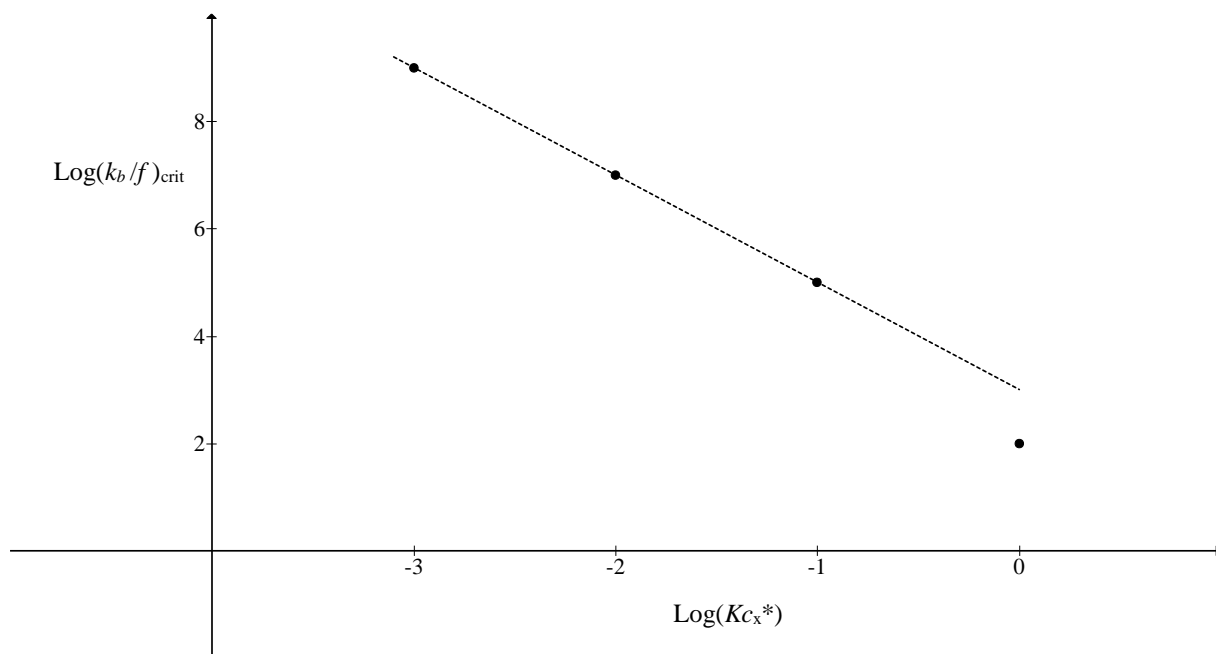
Fig. 8 Dependence of the logarithm of minimum ratio k_b/f that is required for the appearance of the second peak (A) and for the establishment of equilibrium conditions in the ECE mechanism (B) on the logarithm of the product Kc_X^*. Dotted lines in (A) and (B) satisfy eqs. (40) and (42), respectively. All other data are as in Fig. 1.

Conclusions

The main characteristics of the proposed model is the minimum in the relationship between dimensionless net peak current and the dimensionless backward rate constant of chemical reaction. In the models developed on

the assumption that the chemical reaction is totally irreversible, this current decreases sigmoidally with the increasing rate constant. In the general model both forward and backward rate constants are increased proportionally and the ECE mechanism tends to the permanent equilibrium. The characteristics of ECE mechanism can be investigated by the variation of the bulk concentration of the species X^- and the square wave frequency. If the first net peak potential depends on c_X^* and the second one does not, the product Kc_X^* is higher than one. In the opposite case this product is smaller than one. By increasing the frequency the limits of kinetically controlled ECE mechanism can be determined. At the highest frequency the second peak may vanish and the forward rate constant can be estimated using eq. (41) if $Kc_X^* > 10^{-1}$. At the lowest frequency the real net peak currents may depend linearly on the square root of frequency and the slope of the linear relationship between the potential of one of peaks and the logarithm of c_X^* may be -0.059 V. These are indications that either eq. (39) or eq. (42) are satisfied. Under these conditions the equilibrium constant can be measured. The results presented in this paper apply to thermodynamically stable intermediate. If two peaks of ECE mechanism overlap, the effects of frequency and X^- concentration are not clearly visible.

References

1. Laviron, E.; Meunier-Prest, R.; *J. Electroanal. Chem.*, **1992**, *324*, 1-18.

2. Molina, A.; Laborda, E.; Gomez-Gil, J. M.; Compton, R. G.; *J. Solid State Electrochem.*, **2016**, *20*, 3239-3253.

3. Laborda, E.; Gomez-Gil, J. M.; Molina, A.; *Phys. Chem. Chem. Phys.* **2017**, *19*, 16464–16476.

4. Lin, Q.; Li, Q.; Batchelor-McAuley, C.; Compton, R. G.; *J. Phys. Chem. C*, **2015**, *119*, 1489–1495.

5. Gulaboski, R.; Markovski, V.; Jihe, Z.; *J. Solid State Electrochem.*, **2016**, *20,* 3229-3238.

6. Molina, A.; Laborda, E.; Gomez-Gil, J. M.; Martinez-Ortiz, F.; Compton, R. G.; *Electrochim. Acta*, **2016**, *195*, 230–245.

7. Feldberg, S. W.; *J. Phys. Chem.*, **1971**, *75,* 2377-2380.

8. Amatore, C.; Saveant, J. M.; *J. Electroanal. Chem.*, **1978**, *86*, 227-232.

9. Palys, M. J.; Bos, M.; van der Linden, W. E.; *Anal. Chim. Acta*, **1993**, *283*, 811-829.

10. Sanecki, P. T.; Amatore, C.; Skital, P. M.; *J. Electroanal. Chem.*, **2003**, *546*, 109-121.

11. Sanecki, P. T.; Skital, P. M.; *Electrochim. Acta*, **2008**, *53,* 7711-7719.

12. Gulaboski, R.; Mirčeski, V.; Bogeski, I.; Hoth, M.; *J. Solid State Electrochem.*, **2012**, *16*, 2315-2328.

13. Engblom, S. O.; Myland, J. C.; Oldham, K. B.; *Anal. Chem.*, **1994**, *66*, 3182.

14. Galvez, J.; Molina, A.; Saura, R.; Martinez, F.; *J. Electroanal. Chem.,* **1981**, *127*, 17.

15. Amatore, C.; Saveant, J. M.; *J. Electroanal. Chem.,* **1977**, *85*, 27.

16. Mann, M. A.; Helfrick Jr., J. C.; Bottomley, L. A.; *J. Electrochem. Soc.*, **2016**, *163,* H3101-H3109.

17. Miles, A. B.; Compton, R. G.; *J. Electroanal. Chem.*, **2001**, *499,* 1-16.

18. O'Dea, J. J.; Wikiel, K.; Osteryoung, J.; *J. Phys. Chem.*, **1990**, *94,* 3628-3636.

19. Miles, A. B.; Compton, R. G.; *J. Phys. Chem. B*, **2000**, *104,* 5331-5342.

20. Komorsky-Lovrić, Š.; Lovrić, M.; *Anal. Bioanal. Electrochem.*, **2013**, *5,* 291-304.

21. Lovrić, M.; *J. Electrochem. Sci. Eng.,* **2017**, *7*, 119-129.

22. Olmstead, M. L.; Nicholson, R. S.; *J. Electroanal. Chem.*, **1968**, *16,* 145-151.

23. Bieniasz, L. K.; *Modelling Electroanalytical Experiments by the Integral Equation Method*, Springer, Berlin, **2015**.

24. Komorsky-Lovrić, Š.; Lovrić, M.; *Croat. Chem. Acta*, **2017**, *90*, 27-35.